Physics Letters B 704 (2011) 659–662

Contents lists available at SciVerse ScienceDirect

Physics Letters B

www.elsevier.com/locate/physletb

η-Photoproduction in a gauge-invariant chiral unitary framework

Dino Ruić [a], Maxim Mai [a,*], Ulf-G. Meißner [a,b]

[a] Universität Bonn, Helmholtz-Institut für Strahlen- und Kernphysik (Theorie) and Bethe Center for Theoretical Physics, D-53115 Bonn, Germany
[b] Forschungszentrum Jülich, Institut für Kernphysik, Institute for Advanced Simulation, and Jülich Center for Hadron Physics, D-52425 Jülich, Germany

ARTICLE INFO

Article history:
Received 24 August 2011
Received in revised form 21 September 2011
Accepted 23 September 2011
Available online 29 September 2011
Editor: J.-P. Blaizot

Keywords:
Pion–baryon interactions
Photoproduction of η mesons
Baryon resonances

ABSTRACT

We analyze photoproduction of η mesons off the proton in a gauge-invariant chiral unitary framework. The interaction kernel for meson–baryon scattering is derived from the leading order chiral effective Lagrangian and iterated in a Bethe–Salpeter equation. The recent precise threshold data from the Crystal Ball at MAMI can be described rather well and the complex pole corresponding to the $S_{11}(1535)$ is extracted. An extension of the kernel is also discussed.

1. Introduction

Coupled-channel unitary extensions of chiral perturbation theory have been established as a viable tool to investigate the chiral SU(3) dynamics of QCD, for early papers see e.g. [1–5]. The main reason for this is that within such a framework, resonances close to and even below the relevant thresholds can be generated dynamically. The two premier examples are the $\Lambda(1405)$ that features prominently in antikaon–proton scattering and the $S_{11}(1535)$ that dominates the threshold cross section in eta photoproduction off protons. In the context of unitarized chiral perturbation theory, this was first investigated in Refs. [6,7] based on the next-to-leading order (NLO) effective Lagrangian (i.e. using the pertinent contact interactions). The inclusion of p-waves was studied in [8], and the role of the $\pi\pi N$ final-state was investigated in [9]. η and η' photo- and electroproduction based on a U(3) extension of the chiral Lagrangian was considered in [10]. In these groundbreaking papers, the issue of gauge invariance was not considered. In Ref. [11], a gauge-invariant framework for meson photoproduction was developed and applied to associated strangeness production, using the leading order Weinberg–Tomozawa interaction as the driving term in the Bethe–Salpeter equation. In this note, we extend this method to the process $\gamma p \to \eta p$ and in particular to a determination of the mass and width of the $S_{11}(1535)$. Eventually, NLO contributions will have to be included, a first step for the purely hadronic interactions within our approach was recently reported in [12].

2. Framework

In this work we follow the construction procedure of the minimal approach to meson photoproduction, which is exactly unitary in the subspace of meson–baryon channels and gauge-invariant, as developed in Ref. [11]. We refer the reader to that Letter for a more detailed discussion. The first building block of the photoproduction amplitude is the meson–baryon interaction, for which we consider the chiral effective Lagrangian of QCD at leading order:

$$\mathcal{L}^{(1)}_{\phi B} = \langle \bar{B}\big(i\gamma_\mu D^\mu - m_0\big)B\rangle + \frac{D/F}{2}\langle \bar{B}\gamma_\mu\gamma_5\big[u^\mu, B\big]_\pm\rangle, \tag{1}$$

where $\langle\cdots\rangle$ denotes the trace in flavor space, $D_\mu B = \partial_\mu B + [\Gamma_\mu, B]$, m_0 is the baryon octet mass in the chiral SU(3) limit, while D and F are the axial coupling constants. The relevant degrees of freedom are the Goldstone bosons described by the traceless meson matrix $U = u^2 = \exp(i\phi/F_0)$, where F_0 is the meson decay constant in the chiral limit. The meson- and the low-lying baryon-fields are collected in traceless matrices ϕ and B, respectively. Moreover, we use $u^\mu = iu^\dagger(\partial^\mu U - i[v^\mu, U])u^\dagger$ the so-called chiral vielbein. The quark charge matrix is $Q = \mathrm{diag}(2/3, -1/3, -1/3)$, and the external vector field is encoded in $v^\mu = -eQA^\mu$.

The expansion of the chiral connection $\Gamma^\mu = [u^\dagger, \partial_\mu u]/2 - i(u^\dagger v^\mu u + u v^\mu u^\dagger)/2$ in meson fields leads to the meson–baryon vertex of the leading chiral order, the Weinberg–Tomozawa (WT) term. However, at first chiral order, there are also the Born graphs,

* Corresponding author.
E-mail address: mai@hiskp.uni-bonn.de (M. Mai).

0370-2693
doi:10.1016/j.physletb.2011.09.090

describing the s-channel and u-channel exchanges of an intermediate nucleon. The full inclusion of these graphs in the driving term of the Bethe–Salpeter equation (BSE) leads to conceptional and practical difficulties, which have not yet been solved to the best of our knowledge, see [12–14] for a more detailed discussion of this issue. However, most chiral unitary approaches restrict their meson–baryon potential to this interaction, which generates the leading contribution to the s-wave scattering lengths. This approach has been remarkably successful in many cases, thus we iterate the WT-potential $V_{\rm WT} = g(\not{q}_1 + \not{q}_2)$ via the BSE in d space–time dimensions to infinite order as follows

$$T(\not{q}_2, \not{q}_1; p) = V_{\rm WT}(\not{q}_2, \not{q}_1) + \int \frac{d^d l}{(2\pi)^d} V_{\rm WT}(\not{q}_2, \not{l}) iS(\not{p} - \not{l})\Delta(l) T(\not{l}, \not{q}_1; p), \tag{2}$$

where the in-, outgoing meson and the overall four-momentum are denoted by q_1, q_2 and p, respectively. The baryon and the meson propagators are represented by $iS(\not{p}) = i/(\not{p} - m + i\epsilon)$ and $i\Delta(k) = i/(k^2 - M^2 + i\epsilon)$, in order. Moreover, every element of the above equation is a matrix in the channel space. For the case of η-photoproduction considered here, we restrict ourselves to the following channels: $\{p\pi^0, n\pi^+, p\eta, \Lambda K^+, \Sigma^0 K^+, \Sigma^+ K^0\}$.

Because the kernel of the integral Eq. (2) stems from the contact interactions only, we have to deal at most with one-meson–one-baryon loops, which are all dimensionally regularized throughout this work. It is not possible to express the terms necessary to absorb the divergencies in the BSE as counterterms derived from a local Lagrangian. However, it is possible to alter the loop integrals in the solution of the BSE in a way that is in principle equivalent to a proper modification of the chiral potential itself, see [13]. In this spirit we apply the usual $\overline{\rm MS}$ subtraction scheme, keeping in mind that the modified loop integrals are still scale-dependent. This regularization scale (μ) is used as a fitting parameter, reflecting the influence of higher order terms not included in our potential.

The functional form of the driving term allows to construct an explicit solution of the BSE, see [11]. Starting from the corresponding scattering amplitude $T(\not{q}_2, \not{q}_1; p)$, where exact two-body unitarity is guaranteed by construction in the BSE framework, and following the recipe of [11] we are now able to construct the gauge-invariant photoproduction amplitude in a most natural way, without any use of "artificial restoration" of gauge invariance, i.e. adding contact interactions, see e.g. [15,16]. In our approach, we simply couple the photon to any in- and external line as well as to the (momentum-dependent) vertices.

As an intermediate step we construct the amplitude Γ for the process $p \to B\phi$ starting from the potential derived from the leading order Lagrangian Eq. (1) $\hat{V} = \not{q}\gamma_5 \hat{g}$, where q is the outgoing meson momentum and $\hat{g}$ is the (D-, F-dependent) coupling constant corresponding to the second term of Eq. (1). Now we add the loop contribution that accounts for the final state interaction as follows

$$\Gamma(\not{p}, \not{q}) = \hat{V}(\not{q}) + \int \frac{d^d l}{(2\pi)^d} T(\not{q}, \not{l}; p) iS(\not{p} - \not{l})\Delta(l)\hat{V}(\not{l}).$$

Note that the process in question is meson photoproduction off the proton, thus Γ, $\hat{V}$ and $\hat{g}$ are 6-vectors in the channel space.

In the next step we couple the photon in every possible place to the hadronic skeleton. A photon can couple via: $B\phi\gamma \to \phi B$, arising from the chiral connection, $B\gamma \to B$, $\phi\gamma \to \phi$ or via the Kroll–Rudermann interaction $\gamma B \to B\phi$, stemming from the chiral vielbein. These interactions give rise to nine different topologies presented in Fig. 1. Following the conventions of [17] the

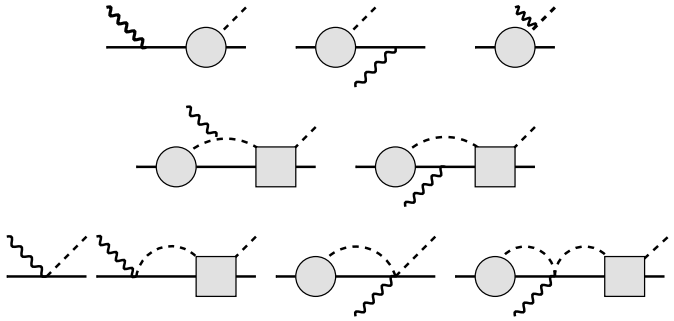

Fig. 1. Different topologies contributing to gauge-invariant photomeson production off the proton. Solid, dashed and wiggly lines denote baryons, mesons and photons, in order. The filled circles/squares denote the meson production/the meson–baryon interaction, i.e. Γ and T, respectively.

most general Lorentz covariant form of the amplitude for the process: $\gamma(k)B_i(p-k) \to B_f(p-q)\phi_f(q)$ can be written as $T_{fi} = i\epsilon_\mu \bar{u}_f(\sum_{i=1}^{8} \mathcal{B}_i \mathcal{N}_i^\mu)u_i$, where ϵ_μ is the photon polarization vector and $u_{i,f}$ are the initial and final Dirac spinors, respectively, which are normalized like $\bar{u}u = 2m$. Moreover $\mathcal{B}$ denote the coefficients of the pseudo-vectors $\mathcal{N}^\mu \epsilon \{\gamma_5\gamma^\mu \not{k}, 2\gamma_5 P^\mu, 2\gamma_5 q^\mu, 2\gamma_5 k^\mu, \gamma_5\gamma^\mu, \gamma_5 \not{k} P^\mu, \gamma_5 \not{k} k^\mu, \gamma_5 \not{k} q^\mu\}$ with $P = 2p - q - k$.

For further study we fix the axis of quantization to the z-axis and rewrite the amplitude once more in terms of CGLN amplitudes and Pauli spinors and matrices as

$$T_{fi} = 8\pi\sqrt{s}\chi_f^\dagger \mathcal{F} \chi_i, \tag{3}$$

where $\mathcal{F} = i(\sigma\cdot\epsilon)\mathcal{F}_1 + (\sigma\cdot\hat{q})(\sigma\cdot[\hat{k}\times\epsilon])\mathcal{F}_2 + i(\sigma\cdot\hat{k})(\hat{q}\cdot\epsilon)\mathcal{F}_3 + i(\sigma\cdot\hat{q})(\hat{q}\cdot\epsilon)\mathcal{F}_4 + i(\sigma\cdot\hat{k})(\hat{k}\cdot\epsilon)\mathcal{F}_5 + i(\sigma\cdot\hat{q})(\hat{k}\cdot\epsilon)\mathcal{F}_6 + i(\sigma\cdot\hat{q})(\hat{k}\cdot\epsilon)\mathcal{F}_6 - i(\sigma\cdot\hat{q})\epsilon_0\mathcal{F}_7 - i(\sigma\cdot\hat{k})\epsilon_0\mathcal{F}_8$ with $\hat{k}$ and $\hat{q}$ normalized three-vectors. For the exact form of CGLN amplitudes in form of coefficients $\mathcal{B}$ we refer the reader to the [11]. Let us note here that due to current conservation two of the eight CGLN amplitudes can be expressed in terms of other six. Moreover two of the remaining six CGLN amplitudes are accompanied by scalar components of ϵ only and thus have no influence on process including real photons. In view on photoproduction this leaves us with four independent CGLN amplitudes.

Let us also mention that by construction of the unitary hadronic interaction the photoproduction amplitude obeys the requirement of two-body unitarity in the subspace of meson–baryon channels automatically. There are five different unitarity classes, which obey the two-body unitarity by themselves. Gauge invariance is, however, fulfilled only if all topologies are taken into account. Note that within the approximation used here, crossing symmetry is violated.

3. Results

We are now able to confront our model with the experimental results, for which we consider the recent measurement of the differential cross sections from the Crystal Ball at MAMI [18]. The parameters of the model are the unknown renormalization scales, whose number is restricted to four due to isospin-symmetry: $\{\mu_{\pi N}, \mu_{\eta N}, \mu_{K\Lambda}, \mu_{K\Sigma}\}$. In contrast to [11] we do not consider the meson decay constants as free parameters, but fix them to their physical values. Our input parameters are: $F_\pi = F_\eta/1.3 = 0.0924$, $F_K = 0.113$, $M_{\pi^0} = 0.135$, $M_{\pi^+} = 0.1396$, $M_\eta = 0.5478$, $M_{K^+} = 0.4937$, $M_{K^0} = 0.4977$, $m_p = 0.9383$, $m_n = 0.9396$, $m_\Lambda = 1.1157$, $m_{\Sigma^0} = 1.1926$, $m_{\Sigma^+} = 1.1894$, $D = 0.8$ and $F = 0.46$ (all masses and decay constants in units of GeV).

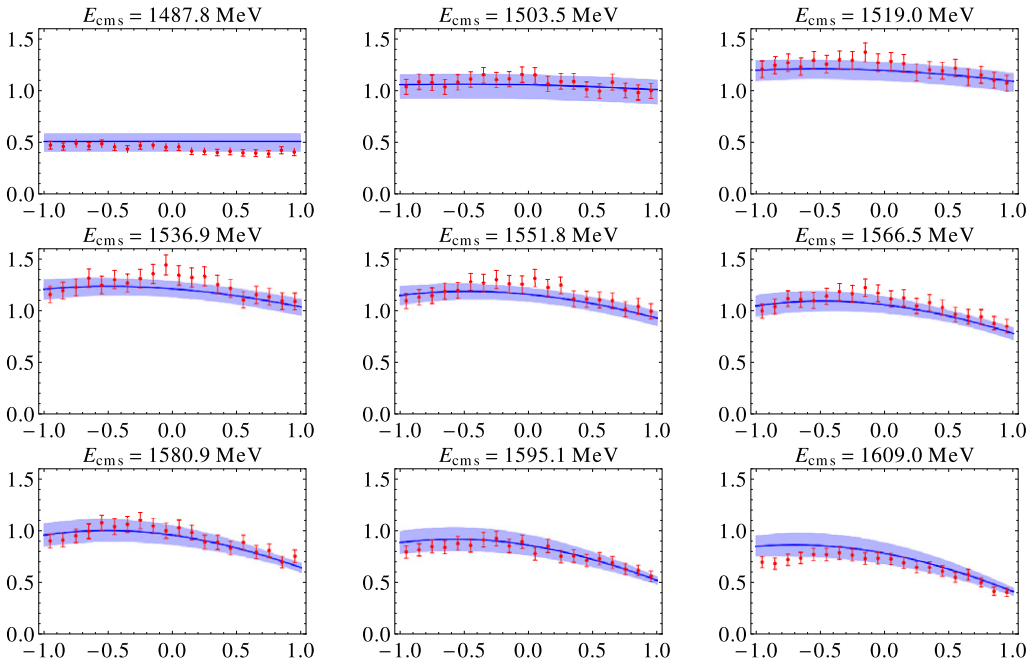

Fig. 2. Best fit of our model (solid lines with shaded error bands) compared to the experimental data from the Crystal Ball at MAMI (filled circles with error bars). The differential cross section $d\sigma/d\Omega$ in [μb/sr] is plotted versus $\cos(\theta)$ for the cms energies given on top of each panel.

The p- and d-waves become important already at moderate energies away from the threshold. Since the kernel of the BSE considered here is the WT-term only, which mainly produces an s-wave contribution, we restrict the center-of-mass (cms) energy of the present analysis to 1487.8 MeV $< E_{\rm cms} <$ 1609.9 MeV. Note that the WT interaction kernel produces a small p-wave contribution via the lower components of the Dirac spinors, however the explicit angular dependence of the amplitude is only described when higher order potentials are taken into account [8]. The calculation of the BSE with the potential at next-to-leading order is performed in Ref. [12] for the hadronic part and is to be extended to photoproduction in Ref. [14]. There the η-photoproduction off the neutron, which is beyond the scope of this work, will also be investigated.

The quality of our fits is given in terms of the $\chi^2_{\rm dof}$,

$$\chi^2_{\rm dof} = \frac{N}{\sigma N - \delta} \sum_E \frac{1}{n(E)} \sum_z \frac{(\frac{d\sigma}{d\Omega}(E,z;\mu) - \frac{d\sigma}{d\Omega}(E,z;e))^2}{(\Delta\frac{d\sigma}{d\Omega}(E,z;e))^2},$$

where $z = \cos(\theta)$, $n(E)$ is the number of data points at energy E, σ is the number of distinct energies and N is the total number of data points. Moreover $\delta = 4$ denotes the number of degrees of freedom, which are called collectively μ. The letter e denotes the experimental values. Using now a random walk minimization procedure, we obtain a $\chi^2_{\rm dof} = 0.9997$ with the following parameters

$$\log(\mu_{\pi N}/\text{GeV}) = -0.611, \qquad \log(\mu_{\eta N}/\text{GeV}) = -0.512^{+0.057}_{-0.051},$$
$$\log(\mu_{K\Sigma}/\text{GeV}) = +1.845, \qquad \log(\mu_{K\Lambda}/\text{GeV}) = -5.112^{+0.403}_{-0.312},$$

where the error bars are obtained by varying the parameters such that the $\chi^2_{\rm dof}$ is increased by one. No uncertainty is given, if it does not affect the value of a parameter at the given accuracy. Some representative differential cross sections are shown in Fig. 2. Quite a good agreement between the model and experiment is achieved for energies more than 100 MeV above threshold, which can be seen from the plot of the integrated cross section in Fig. 3. Above the $K\Lambda$ threshold, the total cross section exceeds the data, this will eventually be overcome in a more precise NLO calculation.

It is commonly believed that the first nucleon resonance, the $S_{11}(1535)$ saturates the cross section close to the ηN threshold. Moreover, it is known that this state can be understood as dynamically generated already from the leading chiral order vertex, i.e. the WT-interaction. Since the latter is also the driving term of our hadronic amplitude it is worth to have a look at the modulus of the electric dipole amplitude E_{0+} as a function of $s = E^2_{\rm cms}$ on the second Riemann sheet. The resonance appears at

$$E_{\rm cms} = \left(1525.9^{+4.4}_{-3.6} - i111.4^{+1.9}_{-2.0}\right) \text{MeV} \tag{4}$$

which is in good agreement with the extraction from phenomenological or other coupled-channel approaches collected in [19] (at least for the real part) and our recent determination from scattering data [12]. It can therefore be identified with the $S_{11}(1535)$ resonance, which is dynamically generated in the present approach. The imaginary part of the pole position is larger than the values of more recent phenomenological approaches collected in [19], however the uncertainty given above reflects only the influence of the errors on the parameters and is certainly underestimated. Moreover this large width is consistent with our determination from scattering at NLO.

For the s-wave multipole E_{0+} we obtain at threshold

$$E_{0+} = \left(-12.39^{+1.51}_{-1.05} + i16.15^{+2.23}_{-1.85}\right) \cdot 10^{-3}/M_{\pi^+}. \tag{5}$$

Its modulus $|E_{0+}| = 20.35^{+2.41}_{-2.38} \cdot 10^{-3}/M_{\pi^+}$ is somewhat larger than the one obtained in the early calculation in unitarized chiral perturbation theory [7] and in certain resonance models including the $S_{11}(1535)$, see e.g. Ref. [20]. Moreover, the ratio of the imaginary to the real part is about 1.06…1.68 and agrees with estimations from resonance models [20].

4. Extension of the model

As stated before, one should include all NLO contributions in the hadronic as well as the electromagnetic part of the production amplitude. However, the full inclusion of such terms is beyond the scope of this work and will be given later [12,14]. As a first

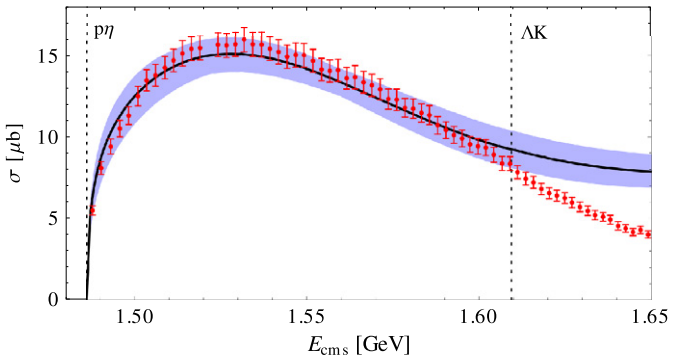

Fig. 3. Total cross section for the best fit of our model (solid lines with shaded error bands) compared to the experimental data from the Crystal Ball at MAMI (filled circles with error bars). The vertical dashed lines denote the $p\eta$ and the $K\Lambda$ thresholds.

step to study the impact of such a modification, it is interesting to consider the magnetic moment couplings of the photon to the nucleon, since these play an important role in phenomenological studies. The corresponding terms of the NLO chiral Lagrangian read [21]

$$b_{12}\langle\bar{B}\sigma^{\mu\nu}\{F^+_{\mu\nu},B\}\rangle + b_{13}\langle\bar{B}\sigma^{\mu\nu}[F^+_{\mu\nu},B]\rangle,$$

where $F^+_{\mu\nu} = uF_{\mu\nu}u^\dagger + u^\dagger F_{\mu\nu}u$ and $F_{\mu\nu} = \partial^\mu v^\nu - \partial^\nu v^\mu$ is the photon field strength tensor. The corresponding additional vertices are restricted to $\gamma B \to B$ and $\gamma B\phi \to B\phi$ only, thus they do not give rise to any change of the hadronic part of our photoproduction amplitude. As a matter of fact unitarity in the subspace of meson–baryon channels is still preserved and the gauge invariance is guaranteed automatically by the functional form of the interaction itself.

Within our model the inclusion of the $b_{12,13}$ terms leads to an additional complication due to the $\Lambda \leftrightarrow \Sigma^0$ transition induced by this terms. Without going into details, see [12,14] for discussion, we have to modify the regularization scheme, such that the pure baryon integrals are set to zero from the beginning. Thus, our treatment of the loop integrals is, in effect, similar to the EOMS regularization scheme advocated in Ref. [22]. Moreover, the same transition implies that $\mu_K = \mu_{K\Sigma} = \mu_{K\Lambda}$, which reduces the original parameter space of our model to $\{\mu_{\pi N}, \mu_{\eta N}, \mu_K, b_{12}, b_{13}\}$.

We have performed fits to the Crystal Ball data on differential cross sections in the same manner as before. However the energy region in question is reduced since no good agreement was achieved even for moderate energies. For the energy region 1487.8 MeV $< E_{\rm cms} <$ 1541.8 MeV we can obtain a fit which minimizes the $\chi^2_{\rm dof}$ to 1.75. For the same regularization scheme, but without the inclusion of $b_{12,13}$ terms we obtain $\chi^2_{\rm dof} = 3.44$. However, the agreement with the data is worse compared to the leading order approach. The conclusion to be drawn is that the inclusion of the Pauli-terms $\sim b_{12,13}$ alone does not improve the LO description. In fact, it is mandatory to perform a full NLO analysis. In particular, as the Pauli coupling is much for important for the neutron, we refrain from giving the LO results for $\gamma n \to \eta n$ here.

5. Summary and outlook

We have shown that the precise data of η-photoproduction in the threshold region can be described rather accurately within the gauge-invariant chiral unitary framework. The $S_{11}(1535)$ resonance is generated dynamically and its pole position in the complex plane agrees with earlier determinations. To go to higher energies, to improve the precision and to investigate also the interesting properties of the same reaction on the neutron, one has to go to NLO and, in the long run, also include the Born terms in the unitarization scheme. Such efforts are under way [14].

Acknowledgements

We are grateful to Peter Bruns for his stimulating remarks and cooperation. We thank Michael Döring for useful discussions. This work is supported in part by the DFG (SFB/TR 16 “Subnuclear Structure of Matter” and SFB/TR 55 “Hadron Physics from Lattice QCD”), by the EU HadronPhysics2 project “Study of Strongly Interacting Matter”, and by the Helmholtz Association through funds provided to the Virtual Institute “Spin and strong QCD” (VH-VI-231).

References

[1] N. Kaiser, P.B. Siegel, W. Weise, Nucl. Phys. A 594 (1995) 325, arXiv:nucl-th/9505043.
[2] E. Oset, A. Ramos, Nucl. Phys. A 635 (1998) 99, arXiv:nucl-th/9711022.
[3] J. Nieves, E. Ruiz Arriola, Nucl. Phys. A 679 (2000) 57, arXiv:hep-ph/9907469.
[4] J.A. Oller, E. Oset, A. Ramos, Prog. Part. Nucl. Phys. 45 (2000) 157, arXiv:hep-ph/0002193.
[5] J.A. Oller, U.-G. Meißner, Phys. Lett. B 500 (2001) 263, arXiv:hep-ph/0011146.
[6] N. Kaiser, P.B. Siegel, W. Weise, Phys. Lett. B 362 (1995) 23, arXiv:nucl-th/9507036.
[7] N. Kaiser, T. Waas, W. Weise, Nucl. Phys. A 612 (1997) 297, arXiv:hep-ph/9607459.
[8] J. Caro Ramon, N. Kaiser, S. Wetzel, W. Weise, Nucl. Phys. A 672 (2000) 249, arXiv:nucl-th/9912053.
[9] T. Inoue, E. Oset, M.J. Vicente Vacas, Phys. Rev. C 65 (2002) 035204, arXiv:hep-ph/0110333.
[10] B. Borasoy, E. Marco, S. Wetzel, Phys. Rev. C 66 (2002) 055208, arXiv:hep-ph/0212256.
[11] B. Borasoy, P.C. Bruns, U.-G. Meißner, R. Nissler, Eur. Phys. J. A 34 (2007) 161, arXiv:0709.3181 [nucl-th].
[12] P.C. Bruns, M. Mai, U.-G. Meißner, Phys. Lett. B 697 (2011) 254, arXiv:1012.2233 [nucl-th].
[13] P.C. Bruns, Ph.D. thesis, Univ. Bonn, 2009, http://hss.ulb.uni-bonn.de/diss_online.
[14] M. Mai, P.C. Bruns, U.-G. Meißner, in press.
[15] H. Haberzettl, C. Bennhold, T. Mart, T. Feuster, Phys. Rev. C 58 (1998) 40, arXiv:nucl-th/9804051.
[16] M. Döring, K. Nakayama, Phys. Lett. B 683 (2010) 145, arXiv:0909.3538 [nucl-th].
[17] F.A. Berends, A. Donnachie, D.L. Weaver, Nucl. Phys. B 4 (1967) 1.
[18] E.F. McNicoll, et al., Crystal Ball at MAMI Collaboration, Phys. Rev. C 82 (2010) 035208, arXiv:1007.0777 [nucl-ex].
[19] K. Nakamura, et al., Particle Data Group Collaboration, J. Phys. G 37 (2010) 075021.
[20] B. Krusche, J. Ahrens, G. Anton, R. Beck, M. Fuchs, A.R. Gabler, F. Haerter, S. Hall, et al., Phys. Rev. Lett. 74 (1995) 3736.
[21] B. Kubis, U.-G. Meißner, Eur. Phys. J. C 18 (2001) 747, arXiv:hep-ph/0010283.
[22] T. Fuchs, J. Gegelia, G. Japaridze, S. Scherer, Phys. Rev. D 68 (2003) 056005, arXiv:hep-ph/0302117.